

1 Title:

2 Divergent extremes but convergent recovery of bacterial and archaeal soil communities to an
3 ongoing subterranean coal mine fire

4

5 Authors:

6 Sang-Hoon Lee^{1,2a}, Jackson W Sorensen^{1a}, Keara L Grady¹, Tammy C Tobin³, and Ashley
7 Shade^{1,4*}

8

9

10 Affiliations:

11 ¹Department of Microbiology and Molecular Genetics, Michigan State University, East Lansing
12 MI 48840

13 ²School of Civil, Environmental, and Architectural Engineering, Korea University, Seoul, South
14 Korea

15 ³Department of Biology, Susquehanna University, Selinsgrove PA 17870

16 ⁴Program in Ecology, Evolutionary Biology, and Behavior, Michigan State University, East
17 Lansing, MI, 48840

18 ^a contributed equally

19 *correspondence: shadeash@msu.edu

20

21 Keywords:

22 press disturbance, microbial diversity, thermophile, soil, community assembly, extremophile,
23 Centralia, resilience, deterministic, stochastic, niche, neutral

24

25 Running title:

26 Stochastic extremes, convergent recovery

27 Abstract

28 Press disturbances are stressors that are extended or ongoing relative to the generation times
29 of community members, and, due to their longevity, have the potential to alter communities
30 beyond the possibility of recovery. They also provide key opportunities to investigate ecological
31 resilience and to probe biological limits in the face of prolonged stressors. The underground coal
32 mine fire in Centralia, Pennsylvania has been burning since 1962 and severely alters the
33 overlying surface soils by elevating temperatures and depositing coal combustion pollutants. As
34 the fire burns along the coal seams to disturb new soils, previously disturbed soils return to
35 ambient temperatures, resulting in a chronosequence of fire impact. We used 16S rRNA gene
36 sequencing to examine bacterial and archaeal soil community responses along two active fire
37 fronts in Centralia, and investigated the influences of assembly processes (selection, dispersal
38 and drift) on community outcomes. The hottest soils harbored the most variable and divergent
39 communities, despite their reduced diversity. Recovered soils converged toward similar
40 community structures, demonstrating resilience within 10-20 years and exhibiting near-complete
41 return to reference communities. Measured soil properties (selection), local dispersal, and
42 neutral community assembly models could not explain the divergences of communities
43 observed at temperature extremes, yet beta-null modeling suggested that communities at
44 temperature extremes follow niche-based processes rather than null. We hypothesize that
45 priority effects from responsive seed bank transitions may be key in explaining the multiple
46 equilibria observed among communities at extreme temperatures. These results suggest that
47 soils generally have an intrinsic capacity for robustness to varied disturbances, even to press
48 disturbances considered to be “extreme”, compounded, or incongruent with natural conditions.

49

50

51 Introduction

52 Human interactions with and alterations of environmental systems are important components of
53 global change (Allen *et al.*, 2014). Anthropogenic disturbances are outcomes of human activity,
54 and include land-use and land-cover changes, pollution, dispersal of invasive species, and over-
55 harvesting of native animal or plant populations (Vitousek *et al.*, 2008). Anthropogenic
56 disturbances are typically classified as press disturbances, as they often impact multiple
57 generations of organisms within their ecosystems (Bender *et al.*, 1984). Because of their

58 longevity, press disturbances have the capacity to alter ecosystems beyond the possibility of
59 recovery (e.g., Thrush *et al.*, 2009).

60 Within every ecosystem, microbial communities underpin biogeochemical processes,
61 sustain the bases of food webs, and recycle carbon and nutrients. In some situations of
62 anthropogenic disturbance, such as pollution, native microbial communities also can provide
63 bioremediative functions to support ecosystem recovery (Ruberto *et al.*, 2009; Desai *et al.*,
64 2010; Ma *et al.*, 2016; Fuentes *et al.*, 2015). Because of their foundational roles in driving
65 important ecosystem processes, understanding how microbial communities respond to press
66 disturbance can provide insights into the potential for ecosystems to recover. It may also help to
67 uncover mechanisms by which environmental microbial communities may be managed to
68 improve ecosystem outcomes. A better understanding of microbial responses to press
69 disturbances, including examples of communities that have recovered or shifted to an
70 alternative stable state, is necessary to move toward the goal of microbial community
71 management (Shade and Peter *et al.*, 2012).

72 Recent work has highlighted the importance of understanding the relative contributions
73 of community assembly processes to community changes (e.g., Vellend, 2010; Nemergut *et al.*,
74 2013; Dini-Andreote *et al.*, 2015; Evans *et al.*, 2016; Vellend *et al.*, 2014; Tucker *et al.*, 2016;
75 Ferrenberg *et al.*, 2013), and these processes can also be informative for understanding
76 community changes after a disturbance (e.g., secondary succession; Dini-Andreote *et al.*,
77 2015). According to Vellend, 2010, community assembly can be summarized by four major
78 processes: dispersal, diversification, drift, and selection. *Dispersal* is the movement of
79 individuals between localities, *diversification* is the generation of new genetic variation (which
80 can lead to speciation), *drift* encompasses the stochastic processes resulting in fluctuations in
81 member abundances (e.g. births and deaths), and *selection* refers to deterministic fitness
82 differences among taxa driven by abiotic conditions or biotic interactions (as summarized by
83 Nemergut *et al.*, 2013). Together, these processes complement and interact to drive community
84 patterns, and together provide a foundation on which to build a predictive theoretical framework
85 for microbial community ecology.

86 Because diversification processes are relatively more important at evolutionary scales,
87 Vellend *et al.* 2014 focused on the remaining processes of ecological selection, drift, and
88 dispersal. They asserted that selection processes are deterministic, that drift processes are
89 stochastic, and that dispersal processes can be either or both, depending on the situation
90 (Vellend *et al.*, 2014). Tucker and colleagues provided clarity to the distinction between

91 deterministic/stochastic and niche/neutral processes, which are often used interchangeably.
92 Niche/neutral refers to the ecological differentiation and equivalence of species, while
93 deterministic/stochastic refers to non-probabilistic or probabilistic outcomes (Tucker *et al.*,
94 2016). Thus, neutrality concerns ecological equivalence of species, while stochasticity concerns
95 demographic variability in birth, death, and dispersal.

96 We aimed to understand the responses of soil microbial communities to an
97 anthropogenic press disturbance, and to apply the Vellend, 2010, Nemergut *et al.*, 2013, and
98 Tucker *et al.*, 2016 conceptual frameworks of community assembly for interpretation of patterns.
99 The town of Centralia, Pennsylvania is the site of an underground coal mine fire that has been
100 burning since 1962. It is one of thousands of coal mine fires burning in the world today (Melody
101 and Johnston, 2015), which are inconspicuously common anthropogenic disturbances.
102 However, the Centralia fire is especially long-lived, and, after efforts to extinguish it failed, it was
103 left to burn until it self-extinguished (Nolter and Vice, 2004). The fire is expected to burn slowly
104 until the coal reserves have been consumed. The fire currently underlies more than 150 acres
105 and continues to spread slowly (3-7 m/yr Elick, 2011) through underground coal seams.
106 Depending on the depth of the coal bed, it burns at an estimated 46-69 m below the surface
107 (Nolter and Vice, 2004; Elick, 2011). Heat, steam and combustion products vent upward from
108 the fire through the overlying soils. The surface soil temperatures can exceed 80°C, scarring the
109 landscape with dead vegetation that reveals the fire's subsurface trajectory. As steam and
110 gasses pass through the overlying rock and soil, soil temperatures increase while soil chemical
111 composition is altered by both spontaneous and microbial-mediated chemical reactions (Janzen
112 and Tobin-Janzen, 2008). As the fire expands into new areas, it also retreats from some
113 affected sites, which then recover to ambient temperatures (Elick, 2011; Nolter and Vice, 2004).
114 Thus, the “end” of the disturbance can be delineated by temperature recovery. In this way, a
115 chronosequence of fire-affected Centralia soils provides a space-for-time proxy of disturbance
116 response and recovery.

117 Our research objectives were to understand the diversity and spatio-temporal dynamics
118 of the surface soil bacterial and archaeal communities that have been impacted historically or
119 are currently influenced by the ongoing subterranean coal mine fire in Centralia. We used a
120 definition of disturbance response to include changes in member relative abundances as well as
121 in composition. Previous work using terminal restriction fragment length polymorphism analysis
122 showed that microbial diversity decreased at hotter sites, and that compositional changes were
123 correlated with soil ammonium and nitrate concentrations (Tobin-Janzen *et al.*, 2005). We move

124 forward from this work to use high throughput sequencing of soil community 16S rRNA genes to
125 quantify the community dynamics along a chronosequence of fire response and recovery. We
126 specifically investigated the community assembly processes of selection, dispersal, and drift.

127

128 **Materials and Methods**

129 *Study site, soil sampling, soil biogeochemistry and microbial community DNA extraction*

130 We undertook fieldwork in Centralia (GPS: 46°46'24"N, 122°50'36"W) on 5-6 October 2014. We
131 collected surface soils to capture the expected maximum changes along a chronosequence of
132 fire recovery (**Supporting Figure 1**). We sampled two fire fronts along gradients of historical fire
133 activity. Fronts are trajectories of fire spread from the 1962 ignition site outward along near-
134 surface coal seams (Elick, 2011). These fronts include surface soils that were previously hot
135 and have cooled, as well as soils that are currently warmed by the ongoing fire. We collected
136 soil from two unaffected, proximate sites as references, seven recovered sites along the
137 gradient, and nine fire-affected sites (18 total soils), and these collections were distributed
138 across both fire fronts. Soil samples were collected from the top 20 cm of surface soil (core
139 diameter 5.1 cm), and were sieved through 4 mm stainless steel mesh. We collected cores only
140 at bare surface soil locations (no vegetation) to minimize the influence of local vegetation and to
141 maximize comparability between soils, as the thermal surface soils generally lacked vegetation.
142 Collected soils were stored on ice up to 72 hr during transport to the laboratory, then stored at -
143 80°C pending further processing. The physico-chemical characteristics of each soil sample
144 (percent moisture, organic matter (500°C), NO₃⁻, NH₄⁺, pH, SO₄, K, Ca, Mg, P, As, and Fe) were
145 assayed by the Michigan State Soil and Plant Nutrient Laboratory according to their standard
146 protocols (East Lansing, MI, USA, <http://www.spnl.msu.edu/>). Gravimetric soil moisture was
147 measured after drying the soil at 80°C for 2 days. Fire history was estimated as years since the
148 surface soil was first hot from the fire, at each sampling location. Fire history observations were
149 measured using either winter snow cover, aerial vegetation photography, or thermal infrared
150 imagery, as collated and reported by Elick, 2011(Figure 3 therein). Soil community DNA was
151 extracted from 0.25 g of soil in three technical replicates using the MoBio Power Soil DNA
152 Isolation Kit according to the manufacturer's protocol (MoBio, Solana Beach, CA, USA). The
153 concentration of the extracted DNA was measured using the Qubit® dsDNA BR Assay Kit (Life
154 Technologies, NY, USA), and DNA amount was standardized for sequencing to 1,000
155 ng/sample.

156

157 *Soil cell counts*

158 Direct bacterial and archaeal cell counts were conducted on frozen soil samples based
159 on a protocol to separate cells from soil reported in (Portillo *et al.*, 2013). To dissociate the
160 microbial cells from soil particles, 10 g of soil was mixed with 100 mL of phosphate buffered
161 saline containing 0.5% Tween-20 (PBST). Soil samples were homogenized in a Waring blender
162 three times for 1 min each, followed by a 5 min incubation on ice. Slurries were centrifuged at
163 1000 x g for 15 min to concentrate soil particulates. Supernatants were set aside and stored at
164 4°C, and the remaining soil pellets were re-suspended in 100 mL of fresh PBST and blended for
165 an additional 1 min. The soil slurry was then transferred to sterile 250 mL centrifuge bottles and
166 the blender was washed with an additional 25 mL of sterile PBST and added to the slurry before
167 centrifugation at 1000 x g for 15 min. All resulting supernatants for each site were combined,
168 then centrifuged at 10,000 x g for 30 min to pellet cells. Supernatants were discarded, and cell
169 pellets were re-suspended in 10 mL of sterile Milli-q water and 400 mL of 37% formaldehyde to
170 fix cells. 1 mL of cell suspension was then carefully layered over 500 µL of sterile Nycodenz
171 solution (0.8 g/mL in 0.85% NaCl), then centrifuged at 10,000 x g for 40 min. The upper layer
172 was then collected and cells were pelleted by centrifugation at 20,000 x g for 15 min, then
173 resuspended in 1 mL of sterile 0.85% NaCl. To dissociate remaining soil clumps, cell
174 suspensions were sonicated for 10 s in a sonicating water bath.

175 Cell suspensions were stained with DTAF ((5-(4,6-Dichlorotriazinyl) Aminofluorescein))
176 according to (Robertson *et al.*, 1999). DTAF-stained smears were visualized on a Nikon Eclipse
177 e800 microscope (Tokyo, Japan) equipped with a Photometrics Coolsnap Myo camera (Tuscon,
178 AZ, USA), and images were collected using Micro-Manager software (Edelstein *et al.*, 2014). Fiji
179 image analysis software was used to adjust background, thresholding, and to conduct particle
180 counts from images (Schindelin *et al.*, 2012). Briefly, background correction was completed
181 using an automated rolling ball subtraction with a 35-pixel radius, followed by automatic local
182 thresholding using the Bernsen method with a 12-pixel radius to convert greyscale images to
183 binary. Watershed segmentation was conducted to separate touching nuclei, then particles were
184 counted using the ImageJ “Analyze Particles” function, excluding anything smaller than 0.1
185 micron (Schneider *et al.*, 2012).

186

187 *Quantitative PCR*

188 We performed quantitative PCR (qPCR) using bacterial and archaeal 16S rRNA gene
189 universal primer sets (**Supporting Table 1**; Caporaso *et al.*, 2012). The reaction mixtures

190 consisted of 10 μ L SYBR qPCR Master mix (Quanta Bioscience, Gaithersburg, MD, USA), 0.4
191 μ L each of the forward and the reverse primers (0.4 pM), 2 μ L of template DNA, and sterilized
192 deionized water to adjust the final volume of 20 μ L. The thermal profile was as follows: initial
193 denaturation at 95°C for 10 s, followed by 40 cycles of denaturation at 95°C for 10 s, annealing
194 at 50°C for 15 s, and extension at 72°C for 40 s. A final dissociation protocol (58°C to 94.5°C,
195 increment 0.5°C for 10 s) was performed to ensure the absence of nonspecific amplicons. The
196 reactions were conducted using the Bio-Rad iQ5 real time detection system (Bio-Rad, Hercules,
197 CA, USA). Please see the supporting materials for more details as to the qPCR methods.

198

199 *16S rRNA amplicon sequencing*

200 For each of the 54 DNA samples (18 soils, each with three replicate DNA extractions) and mock
201 community DNA, paired-end sequencing (150 base pair) was performed on the bacterial and
202 archaeal 16S rRNA gene V4 hypervariable region using the Illumina MiSeq platform (Illumina,
203 CA, USA; **Supporting Table 1**; Caporaso *et al.*, 2012). All of the sequencing procedures,
204 including the construction of Illumina sequencing library using the Illumina TruSeq Nano DNA
205 Library Preparation Kit, emulsion PCR, and MiSeq sequencing were performed by the Michigan
206 State University Genomics Core sequencing facility (East Lansing, MI, USA) following their
207 standard protocols. The Genomics Core provided standard Illumina quality control, including
208 base calling by Illumina Real Time Analysis v1.18.61, demultiplexing, adaptor and barcode
209 removal, and RTA conversion to FastQ format by Illumina Bcl2Fastq v1.8.4. Raw sequences
210 were submitted to the GenBank SRA Accession SRP082686.

211 To estimate sequencing error, mock community DNA was prepared from six different
212 type strains (*D. radiodurans* ATCC13939, *B. thailandensis* E264, *B. cereus* UW85, *P. syringae*
213 DC3000, *F. johnsoniae* UW101, *E. coli* MG1655). The genomic DNA from these type strains
214 were extracted separately using the EZNA Bacterial DNA Kit (Omega Bio-tek, GA, USA)
215 according to the manufacturer's protocol, and then quantified using the Qubit® dsDNA BR
216 Assay Kit (Life Technologies, NY, USA). Each isolates' 16S rRNA sequence was amplified
217 using universal 27F and 1492R primers. Amplification was performed with the GoTaq Green
218 Master Mix (Promega) with the following reaction conditions: 0.4 μ M each primer, 20-200 ng
219 template, 12.5 μ l 2X GoTaq Green Mastermix and nuclease free water to 25 μ L final volume.
220 The products were visualized on 1% agarose gels before being cleaned using the Promega
221 Wizard SV Gel and PCR Cleanup System per manufacturer's instructions. Cleaned
222 amplification products were sequenced using the 27F and 1492R primers using the ABI Prism
223 BigDye Terminator Version 3.1 Cycle kit at Michigan State's Genomics Research Technology

224 Support Facility (<https://rtsf.natsci.msu.edu/genomics/>). Forward and reverse reads were
225 merged using the merger tool in the EMBOSS (V. 6.5.7) package (Rice *et al.*, 2000). Based on
226 the DNA concentration, size of genomic DNA, and 16S rRNA gene copy number, the final
227 mixture contained 100,000 copies of 16S rRNA gene from each strain. The mock community
228 was sequenced alongside the 54 soils' metagenomic DNA. All sequences are available in
229 NCBI's Short Read Archive (<https://www.ncbi.nlm.nih.gov/sra/SRP082686>).

230

231 *Sequence processing*

232 Paired-end sequence merging, quality filtering, denoising, singleton-sequence removal,
233 chimera checking, and open-reference Operational Taxonomic Unit (OTU) picking were
234 conducted using a UPARSE workflow v8.1 (Edgar, 2013; Edgar and Flyvbjerg, 2014). Open-
235 reference OTU picking was modified for compatibility with the UPARSE pipeline but proceeded
236 as described for open-reference workflows (Rideout *et al.*, 2014). We selected open-reference
237 OTU picking because it allowed us to retain all high-quality sequences, even if they did not
238 match to the reference database. In addition, we expected novel diversity in Centralia, and it
239 was likely that many Centralia sequences would not hit to reference databases. Furthermore,
240 we wanted to create consistent OTU definitions that could be tractable across this study and
241 future work. In the open-reference OTU picking workflow, reference-based OTU clustering first
242 was conducted using the `usearch_global` command to cluster sequences with 97% identity to
243 the greengenes database (v 13.8, <http://greengenes.secondgenome.com/downloads>). Second,
244 de novo OTU picking was performed for any sequences that did not hit the greengenes
245 reference; the `usearch` command `cluster_otus` was used to cluster sequences at 97% identity
246 (this step includes chimera checking). The reference-based and de novo OTUs were combined
247 together to create the final dataset. Finally, to reduce the potential effects of candidate
248 contaminant sequences, any sequences in the final dataset that matched 100% to a database
249 of extraneous sequences (found in the mock community) were removed.

250 Additional analyses were performed with QIIME v. 1.9.1 (Caporaso *et al.*, 2010b),
251 including alignment with PyNAST (Caporaso *et al.*, 2010a), taxonomic assignment with the RDP
252 Classifier (Wang *et al.*, 2007), tree building with FastTree (Price *et al.*, 2009),
253 subsampling/rarefaction to an equal sequencing depth, and within and comparative diversity
254 calculations (e.g., UniFrac, Lozupone and Knight, 2005). Sequences identified as Chlorophyta,
255 Streptophyta (i.e., Chloroplasts) and Mitochondria were removed before subsampling to an
256 even sequencing depth. Our sequence analysis workflow and computing notes are available on
257 GitHub

258 (https://github.com/ShadeLab/PAPER_LeeSorensen_inprep/blob/master/Sequence_analysis/MockCommunityWorkflow.md). We used the UPARSE workflow (with the recommended 10%
259 divergence filter) for error rate calculation using the mock community
260 (http://drive5.com/usearch/manual/upp_tut_misop_qual.html).
261

262

263 *Ecological statistics*

264 We first assessed the reproducibility of evenly-sequenced technical replicates (DNA
265 extraction and sequencing replicates), and found that replicates were similar to one another in
266 measures of within-sample (alpha) and comparative diversity (beta diversity). The average and
267 standard deviation of weighted nonnormalized UniFrac distances between replicates was 0.319
268 ± 0.126 with a range from 0.105 to 1.29 (maximum distance between different samples was
269 4.49; **Supporting Figure 2**; and alpha diversity among technical replicates provided in
270 **Supporting Table 2**). Given the low technical variability, unrarefied technical replicates were
271 collapsed into one combined set of sequences for each soil core to provide more exhaustive
272 sequencing of each soil; these collapsed samples were subsampled to an even sequencing
273 depth (321,000 sequences per soil), and singleton OTUs (observed only once in the dataset)
274 were removed before proceeding with analysis. Within sample-diversity of species richness,
275 Faith's phylogenetic diversity (whole tree method), and comparative diversity of weighted and
276 unweighted UniFrac distance (nonnormalized and normalized, (Lozupone *et al.*, 2007; Lozupone
277 *et al.*, 2011) were calculated within QIIME. Non-normalized UniFrac distances can fall outside of
278 0 and 1, while normalized UniFrac distances are bound to 0 to 1; Lozupone *et al.*, 2007 reported
279 no differences in overarching patterns in beta diversity between the nonnormalized and
280 normalized UniFrac (Lozupone *et al.*, 2007), and we have found that this holds for our dataset
281 (**Supporting Table 3**). The data were then moved into the R environment for statistical
282 analyses. Briefly, we used vegan functions for multivariate hypothesis testing, fitting
283 environmental vectors to ordinations (envfit), constrained ordination (capscale), and Mantel
284 tests (mantel) and to calculate Pielou's evenness (Oksanen *et al.*, 2011); the cmdscale function
285 (stats) for principal coordinates analysis; custom code of neutral models of community assembly
286 (Sloan *et al.*, 2007) as written and implemented by Burns *et al.*, 2015 ("sncm.fit_function.R");
287 custom R scripts for beta-null model fitting written by Tucker *et al.*, 2016, Appendix 2 therein)
288 modified by our group to include weighted UniFrac beta-null modeling; and ggplot and ggplots2
289 for plotting (Wickham, 2009). Our R script is available on GitHub ("R_analysis" repository in
290 https://github.com/ShadeLab/PAPER_LeeSorensen_ISMEJ_2017)

291

292

293 **Results and discussion**294 *Soil physical-chemical characteristics and microbial population size*

295 We measured a suite of contextual data for each sampling site, and asked whether any
296 of those data were correlated with surface soil temperature (**Supporting Figure 3**). Centralia
297 soils generally represented a wide range of soil chemistry. We did not find strong correlations
298 between measured contextual data and temperature, with the exception of correlations with
299 ammonium and nitrate (Pearson's $R = 0.50$ and 0.54 , respectively; $p < 0.05$). This finding
300 supports previous work in Centralia showing that ammonium and nitrate were elevated at active
301 vents (Tobin-Janzen *et al.*, 2005). In addition, the pH of recovered sites was consistently lower
302 than reference sites (mean pH = 4.4 and 5.9, respectively), and the hottest soils were more
303 likely to have extreme or disparate values. In two previous reports, soil ammonium, nitrate, and
304 sulfur concentrations were not necessarily correlated with absolute soil temperature values at
305 Centralia, nor to proximity to an active vent; though extreme or disparate chemistry values were
306 sometimes observed at hot sites, values comparable to unaffected sites were also routinely
307 observed (Tobin-Janzen *et al.*, 2005; Janzen and Tobin-Janzen, 2008). The authors suggested
308 that duration of fire impact, whether the fire was advancing or receding from the site, and other
309 complex environmental factors were likely contributing.

310 All soils were within one order of magnitude of 16S rRNA copies per dry mass of soil
311 with fire-affected soils having the highest copy numbers and recovered soils having the lowest,
312 but there were no statistical differences among groups (**Supporting Figure 4A**, Student's t-test
313 all pairwise $p \geq 0.09$). Total number of cells per dry mass of all soil ranged from 10^5 to 10^7 cells
314 per gram of dry soil, but cell counts across fire classifications also were not statistically distinct
315 (**Supporting Figure 4B**, Student's t-test all pairwise $p \geq 0.09$). Together, these data indicate
316 overall community size is relatively stable across the fire gradient and that any changes in
317 community structure along the fire gradient are due to changes in member abundances rather
318 than to differences in the total number of individuals (community size) among soils.

319 Sequencing efforts were near-exhaustive for these soils, as assessed by a clear
320 asymptote achieved with rarefaction (**Supporting Figure 5**). A summary of sequencing efforts,
321 as well as a discussion of reference-based and *de novo* OTU taxonomic assignments for fire-
322 affected and recovered soils, are provided in supporting materials.

323

324 *Selection*

325 To understand the influence of selection (deterministic) processes on community responses, we
326 used surface soil temperatures measured in 2014 to designate categorical groups of
327 communities according to their fire classification. Soils classified as reference and recovered
328 had temperatures between 12 and 15°C (ambient air temperature was 13.3°C at the time of soil
329 collection), while soils classified as fire-affected had temperatures ranging from 21 to 58°C. We
330 hypothesized that within-sample diversity would be lower in fire-affected soils because of the
331 extreme environmental filter of high temperatures, which we expected to result in lower richness
332 and less phylogenetic breadth. Faith's phylogenetic diversity and OTU richness both were
333 lowest and most variable for fire-affected soils, and highest for reference sites (**Figure 1**;
334 Student's t-test all pairwise $p < 0.001$). Pielou's evenness had a similar trend, with fire-affected
335 soils having lower evenness than other soils, suggesting that there are a small number of highly
336 dominant OTUs in the fire-affected soils (all pairwise $p > 0.05$, not significant). These results
337 generally agree with studies investigating soil microbial diversity after coal mine reclamation in
338 China and Brazil, respectively, where the most recovered/reconstructed soils (20 years post-
339 mining in Li *et al.*, 2014) and 19 years of reconstruction in Quadros *et al.*, 2016) had highest
340 within-sample diversity and were most comparable to reference sites. *Centralia* soils are
341 expected to share similar contamination from coal extraction with these mine reclamation soils,
342 but also are distinct because of their thermal conditions and ongoing surface contamination by
343 coal combustion products, such as inorganic gases containing arsenic, selenium, ammonium,
344 sulfur, and hydrogen sulfide, and organic toxins like polycyclic aromatic hydrocarbons (Janzen
345 and Tobin-Janzen, 2008). Elements within inorganic gases mineralize and deposit around active
346 vents (Janzen and Tobin-Janzen, 2008). Some coal combustion products, like volatile sulfur and
347 nitrogen compounds, may enrich for microorganisms capable of using them, while other
348 combustion products, like organic toxins, may decrease microbial community size or diversity
349 (Janzen and Tobin-Janzen, 2008).

350 We used weighted UniFrac distance to assess comparative community diversity across
351 the fire categories. Weighted UniFrac distance was chosen after considering multiple taxonomic
352 and phylogenetic, and weighted and unweighted metrics. All resemblances revealed the same
353 overarching patterns (all pairwise Mantel and PROTEST $p < 0.001$, **Supporting Table 3**),
354 demonstrating that these patterns were very robust. However, weighted UniFrac distance
355 provided the highest explanatory value (**Supporting Table 3**), suggesting that changes in both

356 phylogenetic breadth and the relative abundances of taxa are important for interpreting
357 community responses. As compared to recovered and reference sites, fire-affected soils were
358 distinct (PERMANOVA pseudo $F = 16.10$, $R^2 = 0.50$ and $p = 0.001$ on 1000 permutations) and
359 more variable in their community structure (difference in median dispersions = 0.53, $p = 0.008$;
360 **Figure 2**). Differences in surface soil temperature had most explanatory value on Axis 1 (77.1%
361 variance explained by Axis 1, temperature Axis 1 correlation = 0.97, $p = 0.001$, **Supporting**
362 **Table 4**), with nitrate and iron contributing; calcium and pH (and, to a lesser extent, soil
363 moisture) explained variation on Axis 2 (12.7% variance explained by Axis 2, **Supporting Table**
364 **4**). Notably, soil fire history (estimated years since the local soil surface was first measured hot
365 as reported by Elick, 2011) was not correlated to community dynamics (**Supporting Table 4**).

366 Fire-affected soils were more variable in their community structure across soils,
367 especially in soils at the most extreme temperatures observed (sites C13, C10 which were
368 $>50^{\circ}\text{C}$ at the time of sampling and were at the opposite ends of PCoA2). In contrast, recovered
369 soils were less variable, even though they spanned decades of difference in their years of peak
370 fire activity (the earliest impacted soils that we sampled were last recorded to be hot in 1980;
371 Elick, 2011). Also, recovered soils were very similar in community structure to reference soils.
372 These patterns show that *Centralia* soils achieve divergent community structures over the
373 transition from ambient to extreme conditions, but then generally converge towards a consistent
374 community structure after the fire subsides. These results also show resilience of soil
375 communities impacted by an extreme press disturbance, with recovery occurring within 10-20
376 years after the stressor subsided.

377 We observed a temperature “threshold” effect among fire-affected soils, and soils with
378 temperatures between 21 and 24.5°C (sites C06, C11, and C16) separated cleanly from soils
379 with temperatures greater than 30°C (**Figure 2**). To better understand the divergence in
380 community structure among fire-affected soils, we performed a PCoA with these communities
381 (**Supporting Figure 6A, Supporting Table 5**), and also a constrained analysis to ask what
382 variability remained after removing the influence of temperature (**Supporting Figure 6B,**
383 **Supporting Table 6**). Even after removing the influence of temperature, three discrete subsets
384 of fire-affected communities separated from each other along both axes, with C13 remaining as
385 an outlying point. C13 had very different calcium and pH than the other soils, and both of these
386 factors had high value in discriminating C13 from the other fire-affected soils ($p = 0.092$ and
387 0.014 respectively). There were no other measured abiotic factors that explained the divergence
388 among the fire-affected soils. In addition, the constrained axes had high explanatory value

389 **(Supporting Figure 6B**, combined axes 1 and 2 = 90.0% var. explained), suggesting that,
390 given the measured conditions, there are additional processes beyond abiotic selection that
391 explain the differences in these subsets.

392 We observed broad phylum-level changes in response to the fire (**Figure 3, Supporting**
393 **Table 8**). Not all OTUs affiliated with particular phyla had identical responses; however, our
394 analysis of phylum-level responses points to some general trends. In particular, fire-affected
395 soils were enriched for members of Chloroflexi, Crenarchaeota and many lineages of
396 unidentified Bacteria. As compared to the fire-affected soils, recovered soils also were enriched
397 for Parvarchaeota, Bacteroidetes, Elusimicrobia, Gemmatimonadetes, Planctomycetes,
398 Spirochaetes, TM6, and Verrucomicrobia suggesting that members affiliated with these
399 phyla are able to persist after the fire subsides. Acidobacteria also had an increase in recovered
400 soils (but less significant, $p = 0.10$), presumably because of the decrease in soil pH observed
401 post-fire (**Supporting Figure 3, pH panel: row 1, column 3**). Reference soils had higher
402 representation of Proteobacteria and Verrucomicrobia, which suggests that members of these
403 phyla may be sensitive to the fire.

404

405 *Dispersal and drift*

406 To investigate the relative importance of local dispersal, we assessed the value of spatial
407 distance for explaining differences in community structure. If local dispersal were important, we
408 would expect that soils in close proximity would have more similar community structures than
409 soils that are distant from one another. We found no relationship in the measured spatial
410 distances between soil collection sites and their corresponding differences in community
411 structure for all sites (Mantel $p = 0.66$ on 999 permutations), nor for recovered sites only (after
412 removing the fire-affected sites from analysis; Mantel $p = 0.135$ on 999 permutations). The lack
413 of evidence for spatial autocorrelation suggests that local dispersal is not a key factor shaping
414 community structure in Centralia soils.

415 To explore the relative importance of drift in fire-affected and recovered soils, we used
416 two complementary approaches. First, we fitted a neutral model of community assembly. The
417 model predicts taxon frequencies as a function of their metacommunity log abundances, which
418 is one method to consider the influence of drift with the influence of dispersal (calculated as an
419 immigration term, m , to the model). The neutral model fit better to the recovered sites than to
420 fire-affected sites (R-squared = 0.53, 0.12 respectively; **Supporting Figure 7, Supporting**

421 **Table 7**). Furthermore, we found a lower influence of dispersal (lower value of m) in the fire-
422 affected sites (**Supporting Table 7**). These differences in fit and generally minimal influence of
423 dispersal suggest that neutral processes play a more minor role in the microbial community
424 assembly of fire-affected sites than they do in the recovered sites.

425 Next, we asked how observed differences in beta diversity deviate from null
426 expectations. We used abundance-based beta-null approaches to distinguish niche and null
427 processes according to Tucker *et al.*, 2016, and we extended their approach to also consider
428 community differences in phylogenetic breadth by applying it to weighted UniFrac distances. In
429 this comparative approach, deviations to and from a permuted null expectation (neutral) are
430 used to interpret the relative influences of neutral and niche processes, respectively. All
431 Centralia communities deviated from neutral, with reference and recovered soils falling closer to
432 neutral expectations than fire-affected soils (**Figure 4A**). Fire-affected soils had statistically
433 higher beta-null deviations than recovered soils (both $p < 0.05$ for Bray-Curtis and weighted
434 UniFrac). In the fire-affected soils, there was a consistent increase in niche processes with
435 increasing soil temperature, and the hottest sites deviated furthest from the neutral expectation
436 (**Figure 4B**). Accounting for phylogenetic breadth (using weighted UniFrac distance, **Figure 4B**)
437 suggested relatively less deviation from neutral than accounting for abundance alone (using
438 Bray-Curtis dissimilarity, **Figure 4B**), but both resemblances had similar trends (Pearson's $R =$
439 0.71 , $p = 0.001$) and produced identical statistical outcomes. These abundance null deviation
440 results agree with the Sloan neutral model because they suggest that unmeasured niche
441 processes structure soil communities at temperature extremes.

442

443 *Understanding community divergences at temperature extremes*

444 To dig deeper into the differences in the three subsets of fire-affected soil (**Supporting**
445 **Figure 6**) that were not well explained by measured abiotic selection, local dispersal, or drift as
446 assessed by the Sloan neutral model of community assembly and beta-null modeling, we asked
447 if there were notable differences in their dominant memberships. Fire-affected soils generally
448 had more variability and greater phylogenetic breadth in their dominant membership than
449 recovered soils, and each fire-affected subset harbored an exclusive membership among their
450 most prevalent taxa. We examined the top 10 prevalent taxa from each of the nine fire-affected
451 soils. Collectively, there were 68 unique top 10 OTUs in fire-affected soils (out of a possible 90,
452 if each of the nine fire-affected soil harbored mutually exclusive membership across their top

453 10). These prevalent fire-affected OTUs spanned fourteen phyla or Proteobacteria classes,
454 included 30 *de novo* OTUs, and included seven taxa of unidentified Bacteria and two taxa of
455 unidentified Proteobacteria. Acidobacteria OTUs were detected among the top 10 for all fire-
456 affected soils, and eight of nine fire-affected soils included Chloroflexi among the top 10 OTUs.
457 In comparison, recovered soils included ten phyla or Proteobacteria classes among their
458 collective top 10, had no unidentified Bacteria or Proteobacteria, and included four *de novo*
459 OTUs. Acidobacteria and Alphaproteobacteria OTUs were among the top 10 for all recovered
460 soils, and six of the seven recovered soils also included Deltaproteobacteria. Together, these
461 results show that fire-affected soils were more divergent and diverse in their prevalent
462 membership than recovered soils.

463 An analysis of occurrence patterns of prevalent OTUs also showed greater divergence
464 among fire-affected soils than recovered (**Figure 5**), and further supported the distinction among
465 the subsets of fire-affected soils revealed by the constrained ordination (**Supporting Figure**
466 **6B**). Fire-affected soils had more OTUs within their collective most prevalent taxa, and were
467 more heterogeneous as shown by the wider range represented by the color scale and the more
468 divergent sample and OTU clustering. In fact, taxa that were among the top 10 in one fire-
469 affected soil were likely to be among the rare biosphere in another fire-affected soil, exhibiting
470 stark contrast in their abundances within these soils. However, most of the top 10 prevalent
471 OTUs were detected within every fire-affected soil (**Table 1, Figure 5**), suggesting that changes
472 in taxa relative abundances, rather than turnover in membership, were driving these patterns.

473 This dominance analysis helps to explain the lower fit of the neutral model, and the
474 relatively higher influence of niche processes with beta-null modeling, to fire-affected
475 communities. Outliers to the neutral model that were below detection (taxa that were present in
476 fewer sites than predicted given their relative abundance in the metacommunity) included these
477 many lineages that were prevalent in few fire-affected soils. Taxa that fall below their neutral
478 model prediction have been proposed to be “selected against” or particularly dispersal limited
479 (Burns 2015). However, in the Centralia extreme environment, we suggest these are taxa that
480 were most successful locally given the thermal disturbance.

481

482 *Community assembly processes given a press disturbance*

483 Centralia soil communities were sensitive to the coal mine fire, and changed substantially from
484 reference conditions. Selection processes, specifically abiotic soil conditions, offered high

485 explanatory value for *Centralia* soil community dynamics. These communities first were
486 constrained by environmental filters imposed by the press disturbance, such as thermal
487 temperatures in fire-affected soils and low pH in recovered soils. The fire acts as a strong
488 environmental filter, resulting in decreased diversity and a very different phylogenetic
489 representation among the surviving lineages in fire-affected soils. These environmental filters,
490 such as changes in pH, likely alter the functions of the community as well as its composition.
491 However, even after removing the influence of temperature on fire-affected communities, the
492 communities fell into three distinct subsets that could not be explained by the physico-chemical
493 characteristics measured. Furthermore, neutral modeling, beta-null modeling and lack of spatial
494 autocorrelation suggests that these particular assessments for drift and dispersal processes
495 offer minimal explanation for fire-affected sites. Given the low explanatory value of unweighted
496 resemblances in describing patterns of comparative diversity (**Supporting Table 3**), and the
497 observation that many of the prevalent taxa detected in some fire-affected soils were rare in
498 other fire-affected soils (**Figure 5A**), we can also attribute these patterns to changes in the
499 relative abundances of taxa within a locality, rather than to changes in taxa turnover (differing
500 memberships). Thus, given that neither assessed selection, dispersal, nor drift processes, nor
501 their combination can provide a complete explanation for the divergence of fire-affected
502 communities, the questions remain: why are fire-affected soils so divergent from each other,
503 and how do they eventually manage to recover to the same post-disturbance community
504 structure?

505 One hypothesis is that the remaining variability in community structure of fire-affected
506 sites may be attributed to priority effects initiated from different local transitions between the
507 dormant seed bank and the active community. The proportion of dormant cells in soils is
508 estimated to be as high as 80% (Lennon and Jones, 2011), and the importance of dormancy for
509 microbial community assembly processes has been discussed at length (Nemergut *et al.*, 2013).
510 Specific to the *Centralia* coal mine fire disturbance, thermophiles are prime examples of
511 microbial seed bank members that often have been found in environments that are improbable
512 to permit their growth (e.g., Hubert *et al.*, 2009; McBee and McBee, 1956; Portillo *et al.*, 2012).

513 There are two aspects of seed banks that could help to explain *Centralia* community
514 divergences at temperature extremes: membership and dynamics. If each soil harbored a
515 different seed bank membership, different thermophilic taxa could become active and prevalent
516 in each fire-affected soil, and would manifest as drift influences. This scenario is not well-
517 supported by our data because we detect the dominant members of each fire-affected soil in the

518 other fire-affected soils, albeit in lower abundances. Alternatively, awakenings from the
519 microbial seed bank (Buerger *et al.*, 2012) could result in priority effects at temperature
520 extremes, in which the first fit microorganisms to wake after the fire's local onset have important
521 influence over the community's ultimate trajectory (e.g., Fukami, 2015). In our chronosequence
522 study, the outcome of priority effects would appear as divergent community structures at high
523 temperatures that are explained by niche processes. In addition, unknown nuances in local
524 abiotic conditions at fire onset could also set communities onto parallel trajectories and result in
525 multiple equilibria during the press, which would also be explained by niche processes. Our data
526 indirectly support either of these last two scenarios, as the three separate clusters of fire-
527 affected communities suggest multiple equilibria (**Supporting Figure 6B**). It could be that the
528 most similar fire-affected communities began either from the same (or functionally equivalent)
529 waking pioneer taxon, or from the same abiotic conditions (that are similar beyond reaching
530 thermal temperatures), or from some combination of both, which initiated distinct trajectories
531 towards each equilibrium.

532 Diversification is a fourth community assembly process discussed by Vellend, 2010 and
533 Nemergut *et al.*, 2013. At ecological time scales, diversification was suggested by Vellend *et al.*,
534 2014 to have relatively lower influence than the other community assembly processes. We do
535 not directly address diversification in this study, focusing instead on ecological processes. Aside
536 from a consistent observation of Acidobacteria and Chloroflexi among the dominant taxa in fire-
537 affected soils, there is no evidence that different but closely related lineages are most prevalent
538 across all fire-affected soils, which may have hinted at distinct but parallel trajectories of
539 diversification within a locality. However, we cannot reject the hypothesis that diversification
540 processes also contribute to divergences in community structure at temperature extremes.

541

542 *Conceptual model*

543 Extending the conceptual models of Ferrenberg *et al.*, 2013 and Dini-Andreote *et al.*,
544 2015, we present a hypothesis of the assembly processes shaping communities before, during,
545 and after an extreme press disturbance. Our model is based on our chronosequence trajectory
546 for beta-null data presented in **Figure 4B**, and includes a phase encompassing the press
547 disturbance, which extends beyond the representation of a pulse disturbance as a single time
548 point as typical in previous conceptual models. Our model also incorporates a hypothesis of
549 multiple transient equilibria within the press disturbance phase. We apply the advice of (Tucker

550 *et al.*, 2016) to not use the direction of the change from neutral (positive or negative) to infer
551 specific ecological processes.

552 We hypothesize that weak variable selection drives stability in heterogeneous Centralia
553 soil communities before the fire (reference sites in **Figure 4**; phase 1 in **Figure 6**). This is
554 additionally supported by the literature demonstrating generally high heterogeneity and diversity
555 in mature soil microbial communities (*e.g.*, O'Brien *et al.*, 2016). Next, strong environmental
556 filtering from thermal temperatures (homogeneous selection, phase 2) decreases community
557 diversity at the onset of the press disturbance. The lower diversity and prolonged disturbance
558 conditions permit priority effects initiated by taxa fit in the thermal environment (*e.g.*,
559 thermophiles waking from the seedbank), which set communities onto distinct deterministic
560 trajectories with multiple equilibria during the fire (phase 2). Alternatively, the distinct trajectories
561 and multiple equilibria could have been initiated by unmeasured nuances in abiotic conditions at
562 thermal onset. Finally, weak environmental filtering from increased soil acidity relaxes
563 communities back towards neutral in post-fire conditions (homogeneous selection, phase 3).

564 Regardless of the interim dynamics that resulted in community divergence to the
565 stressor, Centralia soils eventually recovered to a community structure very similar to reference
566 soils, and these community structures were explained by the ultimate post-fire soil environment.
567 Our results show that Centralia soil communities, though sensitive to this extreme, complex, and
568 arguably unnatural stressor, had near-complete return to pre-disturbance conditions, and were
569 resilient within ten to twenty years after the stressor subsides. We have no reason to suspect
570 that temperate soils in Centralia are exceptional as compared to other soils. Thus, these results
571 suggest that soils may have an intrinsic capacity for robustness to varied disturbances, even to
572 those disturbances considered to be “extreme”, compounded, or incongruent with natural
573 conditions. Understanding the precise functional underpinnings of soil microbial community
574 resilience, including the roles of seed banks in determining that resilience, is a next important
575 step in predicting and, potentially, managing, microbial community responses to disturbances.

576

577 **Acknowledgements**

578

579 This work was supported by Michigan State University, with computing resources provided by
580 the Michigan State Institute for Cyber-Enabled Research. JWS acknowledges the Dr. C. A.

581 Reddy and Sasikala Reddy Award from the Michigan State Department of Microbiology and
582 Molecular Genetics. We thank Trevor Grady for his graphic design work for Supporting Figure 1.

583

584 **Conflict of Interest Statement**

585 The authors declare no conflict of interest.

586

587 **References**

588 Allen MR, Barros VR, Broome J, Cramer W, Christ R, Church JA, *et al.* (2014). IPCC Fifth
589 Assessment Synthesis Report-Climate Change 2014 Synthesis Report. *IPCC Fifth Assess*
590 *Synth Report-Climate Chang 2014 Synth Rep* pages: 167.

591 Bender EEA, Case TJJ, Gilpin ME. (1984). Perturbation Experiments in Community Ecology:
592 Theory and Practice. *Ecology* **65**: 1–13.

593 Buerger S, Spoering A, Gavrish E, Leslin C, Ling L, Epstein SS. (2012). Microbial scout
594 hypothesis, stochastic exit from dormancy, and the nature of slow growers. *Appl Environ*
595 *Microbiol* **78**: 3221–3228.

596 Burns AR, Zac Stephens W, Stagaman K, Wong S, Rawls JF, Guillemin K, *et al.* (2015).
597 Contribution of neutral processes to the assembly of gut microbial communities in the zebrafish
598 over host development. *Isme J* 1–10.

599 Caporaso JG, Bittinger K, Bushman FD, DeSantis TZ, Andersen GL, Knight R. (2010a).
600 PyNAST: a flexible tool for aligning sequences to a template alignment. *Bioinformatics* **26**: 266–
601 267.

602 Caporaso JG, Kuczynski J, Stombaugh J, Bittinger K, Bushman FD, Costello EK, *et al.* (2010b).
603 QIIME allows analysis of high-throughput community sequencing data. *Nature* **7**: 335–336.

604 Caporaso JG, Lauber CL, Walters W a, Berg-Lyons D, Huntley J, Fierer N, *et al.* (2012). Ultra-
605 high-throughput microbial community analysis on the Illumina HiSeq and MiSeq platforms. *ISME*
606 *J* **6**: 1621–1624.

607 Caporaso JG, Lauber CL, Walters WA, Berg-Lyons D, Lozupone CA, Turnbaugh PJ, *et al.*
608 (2011). Global patterns of 16S rRNA diversity at a depth of millions of sequences per sample.
609 *Proc Natl Acad Sci U S A* **108**: 4516.

610 Desai C, Pathak H, Madamwar D. (2010). Advances in molecular and ‘-omics’ technologies to
611 gauge microbial communities and bioremediation at xenobiotic/anthropogen contaminated sites.

- 612 *Bioresour Technol* **101**: 1558–1569.
- 613 Dini-Andreote F, Stegen JC, van Elsas JD, Salles JF. (2015). Disentangling mechanisms that
614 mediate the balance between stochastic and deterministic processes in microbial succession.
615 *Proc Natl Acad Sci* **112**: E1326–E1332.
- 616 Edelstein AD, Tsuchida M a, Amodaj N, Pinkard H, Vale RD, Stuurman N. (2014). Advanced
617 methods of microscope control using µManager software. *J Biol Methods* **1**: 10.
- 618 Edgar RC. (2013). UPARSE: highly accurate OTU sequences from microbial amplicon reads.
619 *Nat Methods* **10**: 996–8.
- 620 Edgar RC, Flyvbjerg H. (2014). Error filtering, pair assembly and error correction for next-
621 generation sequencing reads. *Bioinformatics* **31**: 3476–3482.
- 622 Elick JM. (2011). Mapping the coal fire at Centralia, Pa using thermal infrared imagery. *Int J*
623 *Coal Geol* **87**: 197–203.
- 624 Evans S, Martiny JB, Allison SD. (2016). Effects of dispersal and selection on stochastic
625 assembly in microbial communities. *ISME J* 1–10.
- 626 Ferrenberg S, O'Neill SP, Knelman JE, Todd B, Duggan S, Bradley D, *et al*. (2013). Changes in
627 assembly processes in soil bacterial communities following a wildfire disturbance. *Isme J* **7**:
628 1102–1111.
- 629 Fuentes S, Barra B, Gregory Caporaso J, Seeger M. (2015). From rare to dominant: A fine-
630 tuned soil bacterial bloom during petroleum hydrocarbon bioremediation. *Appl Environ Microbiol*
631 **82**: 888–896.
- 632 Fukami T. (2015). Historical contingency in community assembly : integrating niches, species
633 pools, and priority effects. *Annu Rev Ecol Evol Syst* **46**: 1–23.
- 634 Hubert C, Loy a., Nickel M, Arnosti C, Baranyi C, Bruchert V, *et al*. (2009). A Constant Flux of
635 Diverse Thermophilic Bacteria into the Cold Arctic Seabed. *Science (80-)* **325**: 1541–1544.
- 636 Janzen C, Tobin-Janzen T. (2008). Microbial Communities in Fire-Affected Soils. In:
637 *Microbiology of Extreme Soils*. Springer, pp 299–316.
- 638 Lennon JT, Jones SE. (2011). Microbial seed banks: the ecological and evolutionary
639 implications of dormancy. *Nat Rev Microbiol* **9**: 119–130.
- 640 Li Y, Wen H, Chen L, Yin T. (2014). Succession of bacterial community structure and diversity in
641 soil along a chronosequence of reclamation and re-vegetation on coal mine spoils in China.

- 642 *PLoS One* **9**. e-pub ahead of print, doi: 10.1371/journal.pone.0115024.
- 643 Lozupone CA, Hamady M, Kelley ST, Knight R. (2007). Quantitative and qualitative diversity
644 measures lead to different insights into factors that structure microbial communities. *Appl*
645 *Environ Microbiol* **73**: 1576–1585.
- 646 Lozupone C, Knight R. (2005). UniFrac: a new phylogenetic method for comparing microbial
647 communities. *Appl Environ Microbiol* **71**: 8228–8235.
- 648 Lozupone C, Lladser ME, Knights D, Stombaugh J, Knight R. (2011). UniFrac: an effective
649 distance metric for microbial community comparison. *ISME J* **5**: 169–172.
- 650 Ma Y, Rajkumar M, Zhang C, Freitas H. (2016). Beneficial role of bacterial endophytes in heavy
651 metal phytoremediation. *J Environ Manage* **174**: 14–25.
- 652 MCBEE RH, MCBEE VH. (1956). The incidence of thermophilic bacteria in arctic soils and
653 waters. *J Bacteriol* **71**: 182–187.
- 654 Melody S, Johnston F. (2015). Coal mine fires and human health: What do we know? *Int J Coal*
655 *Geol* **152**: 1:14.
- 656 Nemergut DR, Schmidt SK, Fukami T, O'Neill SP, Bilinski TM, Stanish LF, *et al*. (2013).
657 Patterns and Processes of Microbial Community Assembly. *Microbiol Mol Biol Rev* **77**: 342–356.
- 658 Nolter M a, Vice DH. (2004). Looking back at the Centralia coal fire: a synopsis of its present
659 status. *Int J Coal Geol* **59**: 99–106.
- 660 O'Brien SL, Gibbons SM, Owens SM, Hampton-Marcell J, Johnston ER, Jastrow JD, *et al*.
661 (2016). Spatial scale drives patterns in soil bacterial diversity. *Environ Microbiol* **18**: 2039–2051.
- 662 Oksanen AJ, Blanchet FG, Kindt R, Minchin PR, Hara RBO, Simpson GL, *et al*. (2011). vegan :
663 community ecology package. *R Packag version 115-1*. <http://cran.r-project.org/>, <http://vegan.r-forge.r-project.org>.
- 665 Portillo MC, Leff JW, Lauber CL, Fierer N. (2013). Cell size distributions of soil bacterial and
666 archaeal taxa. *Appl Environ Microbiol* **79**: 7610–7617.
- 667 Portillo MC, Santana M, Gonzalez JM. (2012). Presence and potential role of thermophilic
668 bacteria in temperate terrestrial environments. *Naturwissenschaften* **99**: 43–53.
- 669 Price MN, Dehal PS, Arkin AP. (2009). FastTree: Computing large minimum evolution trees with
670 profiles instead of a distance matrix. *Mol Biol Evol* **26**: 1641–1650.
- 671 Quadros PD de, Zhalnina K, Davis-Richardson AG, Drew JC, Menezes FB, Camargo FA d. O,

- 672 *et al.* (2016). Coal mining practices reduce the microbial biomass, richness and diversity of soil.
673 *Appl Soil Ecol* **98**: 195–203.
- 674 Rice P, Longden I, Bleasby A. (2000). EMBOSS: The European Molecular Biology Open
675 Software Suite. *Trends Genet* **16**: 276–277.
- 676 Rideout JR, He Y, Navas-Molina JA, Walters WA, Ursell LK, Gibbons SM, *et al.* (2014).
677 Subsampled open-reference clustering creates consistent, comprehensive OTU definitions and
678 scales to billions of sequences. *PeerJ* **2**: e545.
- 679 Robertson GP, Coleman DC, Bledsoe C (eds). (1999). Standard Soil Methods for Long-Term
680 Ecological Research. Oxford University Press: Cary, NC, USA.
- 681 Ruberto L, Dias R, Lo Balbo A, Vazquez SC, Hernandez EA, Mac Cormack WP. (2009).
682 Influence of nutrients addition and bioaugmentation on the hydrocarbon biodegradation of a
683 chronically contaminated Antarctic soil. *J Appl Microbiol* **106**: 1101–1110.
- 684 Schindelin J, Arganda-Carreras I, Frise E, Kaynig V, Longair M, Pietzsch T, *et al.* (2012). Fiji: an
685 open source platform for biological image analysis. *Nat Methods* **9**: 676–682.
- 686 Schneider C a, Rasband WS, Eliceiri KW. (2012). NIH Image to ImageJ: 25 years of image
687 analysis. *Nat Methods* **9**: 671–675.
- 688 Shade A, Peter H, Allison SD, Baho D, Berga M, Buergmann H, *et al.* (2012). Fundamentals of
689 microbial community resistance and resilience. *Front Microbiol* **3**: 417.
- 690 Sloan WT, Woodcock S, Lunn M, Head IM, Curtis TP. (2007). Modeling taxa-abundance
691 distributions in microbial communities using environmental sequence data. In: Vol. 53. *Microbial*
692 *Ecology*. pp 443–455.
- 693 Thrush SF, Hewitt JE, Dayton PK, Coco G, Lohrer AM, Norkko A, *et al.* (2009). Forecasting the
694 limits of resilience: integrating empirical research with theory. *Proc R Soc B Biol Sci* **276**: 3209–
695 3217.
- 696 Tobin-Janzen T, Shade A, Marshall L, Torres K, Beblo C, Janzen C, *et al.* (2005). Nitrogen
697 Changes and Domain Bacteria Ribotype Diversity in Soils Overlying the Centralia, Pennsylvania
698 Underground Coal Mine Fire. *Soil Sci* **170**: 191–201.
- 699 Tucker CM, Shoemaker LG, Davies KF, Nemergut DR, Melbourne BA. (2016). Differentiating
700 between niche and neutral assembly in metacommunities using null models of β -diversity. *Oikos*
701 **125**: 778–789.

- 702 Vellend M. (2010). Conceptual synthesis in community ecology. *Q Rev Biol* **85**: 183–206.
- 703 Vellend M, Srivastava DS, Anderson KM, Brown CD, Jankowski JE, Kleynhans EJ, *et al*. (2014).
704 Assessing the relative importance of neutral stochasticity in ecological communities. *Oikos* **123**:
705 1420–1430.
- 706 Vitousek PM, Mooney HA, Lubchenco J, Melillo JM. (2008). Human domination of Earth's
707 ecosystems. In: *Urban Ecology: An International Perspective on the Interaction Between*
708 *Humans and Nature*. pp 3–13.
- 709 Wang Q, Garrity GM, Tiedje JM, Cole JR. (2007). Naive Bayesian classifier for rapid
710 assignment of rRNA sequences into the new bacterial taxonomy. *Appl Environ Microbiol* **73**:
711 5261–5267.
- 712 Wickham H. (2009). *ggplot2: elegant graphics for data analysis*. Springer: New York.
- 713

714 **Figures**

715 **Figure 1.** Within-sample (alpha) diversity of fire-affected, recovered, and reference soils in
716 Centralia for bacterial and archaeal community **(A)** Faith's phylogenetic diversity (all $p < 0.001$);
717 **(B)** richness (total no. observed OTUs clustered at 97% sequence identity, all $p < 0.001$); and
718 **(C)** Pielou's evenness (all p not significant).

719 **Figure 2.** Principal coordinate analysis (PCoA) based on weighted UniFrac distances of
720 phylogenetic bacterial and archaeal community structure. Colors show the fire classification of
721 the soil as fire-affected (red), recovered (yellow), or reference (green). The strength of
722 statistically significant ($p < 0.10$) explanatory variables are shown with solid arrows.

723 **Figure 3.** Phylum-level responses to the Centralia coal mine fire. Mean relative abundance of
724 phyla summarized within soil fire classifications (fire-affected, recovered, and reference).
725 Unidentified Bacteria are a combination of OTUs unable to be assigned taxonomy at the phylum
726 level, and are not a monophyletic group. "Phyla Below 0.01" are all OTUs assigned to phyla that
727 collectively comprise less than 0.01 relative abundance in, and also are not a monophyletic
728 group.

729 **Figure 4.** The relative changes in niche and neutral processes assessed using deviations from
730 abundance-weighted beta-null models. Color gradient shows the soil temperature, as a proxy
731 for disturbance intensity. **(A)** Abundance null deviations by fire classification. For both Bray-
732 Curtis and weighted Unifrac resemblances, recovered and fire-affected communities had distinct
733 null deviations (both $p < 0.05$); **(B)** Trajectory of beta-null deviations ranked by disturbance
734 intensity from reference to fire-affected to recovered soils. Weighted UniFrac and Bray-Curtis
735 trajectories are correlated ($p = 0.71$, $p = 0.001$).

736 **Figure 5.** Relative abundances of the collection of the most prevalent combined "top 10" taxa
737 (rows) observed in **(A)** fire-affected or **(B)** recovered soils (columns) in Centralia. Color
738 gradients indicate taxa relative abundances, with warm colors indicating prevalent taxa and cool
739 colors indicating rare taxa within that soil. Note differences in color scale gradient between **(A)**
740 and **(B)**. Column labels are sample IDs, and OTU IDs are provided as row labels. OTU IDs that
741 begin "OTU_dn" indicate that the taxon was clustered *de novo* in the open-reference OTU
742 picking workflow; IDs that are numeric indicate that the taxon was assigned with high identity to
743 a reference in the greengenes database. For reference-based OTUs, the numeric identifier
744 corresponds to its representative sequence in the greengenes database. Top dendrograms

745 cluster soils that have similar community structure, and side dendrograms cluster OTUs that
746 have similar occurrence patterns.

747 **Figure 6.** Hypothesized conceptual model of *Centrilia* community assembly following press
748 disturbance. Phase 1 represents the stable soil community pre-fire, and is characterized by
749 weak variable selection from typical soil heterogeneity and high community diversity. Because
750 the disturbance is a press, phase 2 occurs concurrent with the fire, when strong environmental
751 filters (homogenizing selection) imposed by the extreme conditions drive a sharp increase in
752 niche processes away from neutral conditions at the onset of the fire. Within phase 2, multiple
753 equilibria result from priority effects of pioneer taxa that are fit to survive in the extreme press
754 environment. Phase 3 is post-fire, characterized by relatively weak environmental filtering (e.g.,
755 increased in soil acidity) that relaxes communities towards neutral. Complete neutrality was not
756 observed in pre-fire or post-fire soils.

757

758

759 **Tables**

760 **Table 1.** Ten most abundant OTUs in fire-affected Centralia soils. OTUs (defined at 97%
761 sequence identity) were assigned to the most resolved taxonomic level possible; there were no
762 taxonomic assignments that could be made to these prevalent OTUs below the family level
763 (RDP Classifier confidence > 0.80).
764

765 **Supporting Figures**

766 **Supporting Figure 1.** Soil sampling sites at Centralia mine fire. In total, 18 surface soil samples
767 (5.08 cm x 20 cm PVC core) were collected along two fire fronts in Centralia, on 15/16 October
768 2014. Sampling sites encompass a gradient of historical fire activity (red flags: Fire-affected in
769 2014 (temperature > 21°C); yellow flags: recovered in temperature, post-fire; and green flags:
770 reference soils).

771 **Supporting Figure 2.** PCoA showing the variability among technical replicates. Three replicate
772 DNA extractions, amplifications and sequencing reactions were performed per soil, and these
773 sequences were subsequently pooled into one aggregate set of sequences to achieve deep
774 coverage of the community within each soil. Error bars are standard deviation around the mean
775 weighted UniFrac distance among technical replicates, each subsampled to an even 53,000
776 sequences per replicate.

777 **Supporting Figure 3.** Soil physical and chemical contextual data (x-axis) plotted against
778 temperature (y-axis). Color gradient shows the soil temperature, and symbols show soil fire
779 classification in October 2014 as fire-affected, recovered, or reference.

780 **Supporting Figure 4.** Quantification of **(A)** 16S rRNA copies per gram of dry soil and **(B)** cell
781 counts per gram of dry soil in fire-affected, recovered, and reference soils. 16S rRNA copies
782 were assessed using quantitative PCR, and cell counts were assessed using cell separation
783 from soil, staining and microscope imaging. There were no statistical differences in values
784 across fire classification for either measurement (all pairwise $p > 0.09$ with a student's t-test).

785 **Supporting Figure 5.** Centralia 16S rRNA amplicon sequencing effort assessed by
786 subsampling/rarefaction of **(A)** richness and **(B)** Faith's phylogenetic diversity with increasing
787 total number of sequences.

788 **Supporting Figure 6.** Divergences in fire-affected soils are not well explained by temperature.
789 **(A)** Principal coordinate analysis (PCoA) based on weighted UniFrac distances of phylogenetic
790 bacterial and archaeal community structure in fire-affected soils. The strength of statistically
791 significant ($p < 0.10$) explanatory variables are shown with blue arrows. **(B)** Constrained
792 analysis (CAP) based on weighted UniFrac distances, where the explanatory value of
793 temperature is removed from the analysis to understand the influence of the remaining
794 explanatory variables.

795 **Supporting Figure 7.** Neutral models of community assembly (abundance v. occurrence) for
796 (A) the total community (“All”, n= 18), (B) recovered soils (“Recovered” n=7), and (C) fire-
797 affected soils (“Fire_Affected”, n=9). (Red symbols show OTUs that had higher abundance than
798 their prediction, and blue symbols show OTUs that had lower abundance than their prediction.
799 The thick yellow line is the neutral model prediction, and the thin yellow lines show a 95%
800 confidence interval around the prediction.

801 **Supporting Figure 8.** Quantitative PCR standard curve for the amount of *E.coli* 16S rRNA
802 gene copies (cloned into plasmids) versus C_T values. The solid line is the regression ($R^2 =$
803 0.988). The error bars are the standard deviations obtained in three independent experiments.
804

805 **Supporting Tables**

806 **Supporting Table 1.** Primers used in this study.

807 **Supporting Table 2.** Mean and standard deviation (“sd”) of phylogenetic diversity and number
808 of OTUs (“richness”) across technical sequencing replicates for the un-collapsed dataset
809 (rarefied to 53,000 sequences per sample). Three replicate DNA extractions, amplifications and
810 sequencing reactions were performed per soil, and, after calculating the technical variability,
811 these sequences were pooled into one aggregate set of sequences to achieve deep coverage
812 of the community within each soil.

813 **Supporting Table 3.** (A) Percent variation explained for PCoA axes 1 and 2 for nonnormalized
814 weighted and unweighted UniFrac, normalized weighted UniGrac, Sorensen-dice, and Bray-
815 Curtis distances/dissimilarities. Nonnormalized weighted UniFrac was chosen because it was
816 most informative in explaining the variance along the first two axes. (B) Pairwise resemblance
817 correlations calculated with Mantel and PROTEST. All $p < 0.001$ for all tests.

818 **Supporting Table 4.** Explanatory value of soil contextual data to changes in Centralia soil
819 community structure along PCoA axes for the all soils. Factors significant at $p < 0.10$ are in
820 bold.

821 **Supporting Table 5.** Explanatory value of soil contextual data to changes in Centralia soil
822 community structure along PCoA axes for the fire-affected soils. Factors significant at $p < 0.10$
823 are in bold.

824 **Supporting Table 6.** Explanatory value of soil contextual data to changes in *Centralia* soil
825 community structure along the constrained PCoA axes for the fire-affected soils, after removing
826 the influence of temperature. Factors significant at $p < 0.10$ are in bold.

827 **Supporting Table 7.** Parameters and fits of neutral models, implemented as per Burns et al.
828 2015.

829 **Supporting Table 8.** Welch's t-tests comparing the mean relative abundances of phyla across
830 fire-affected and recovered soils. Bold values are significant at $p < 0.05$.

831

832

Figure 1

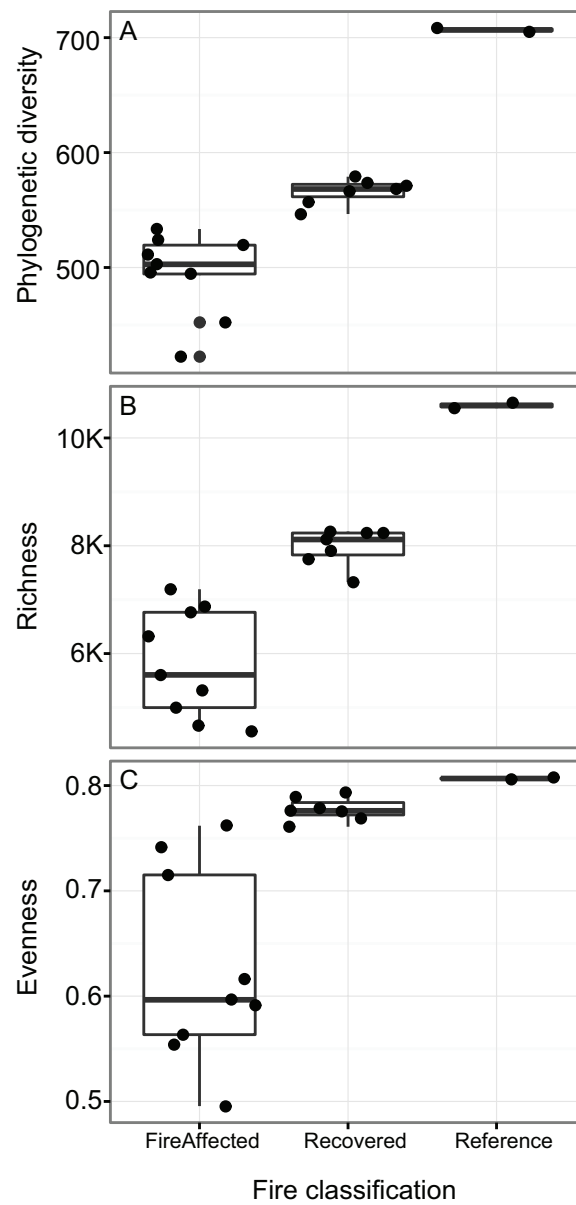


Figure 2

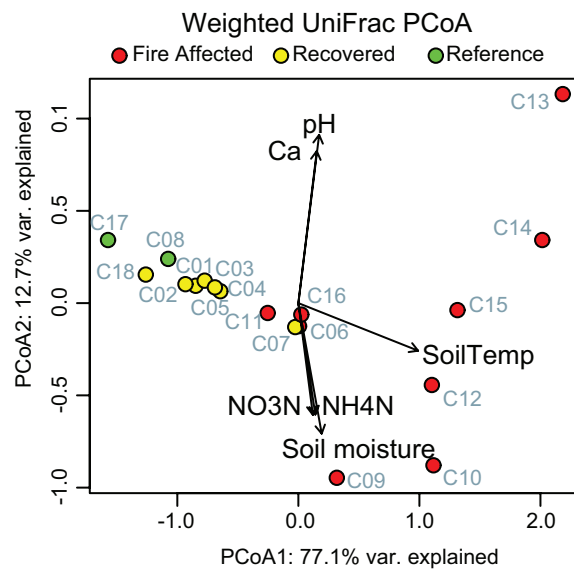


Figure 3

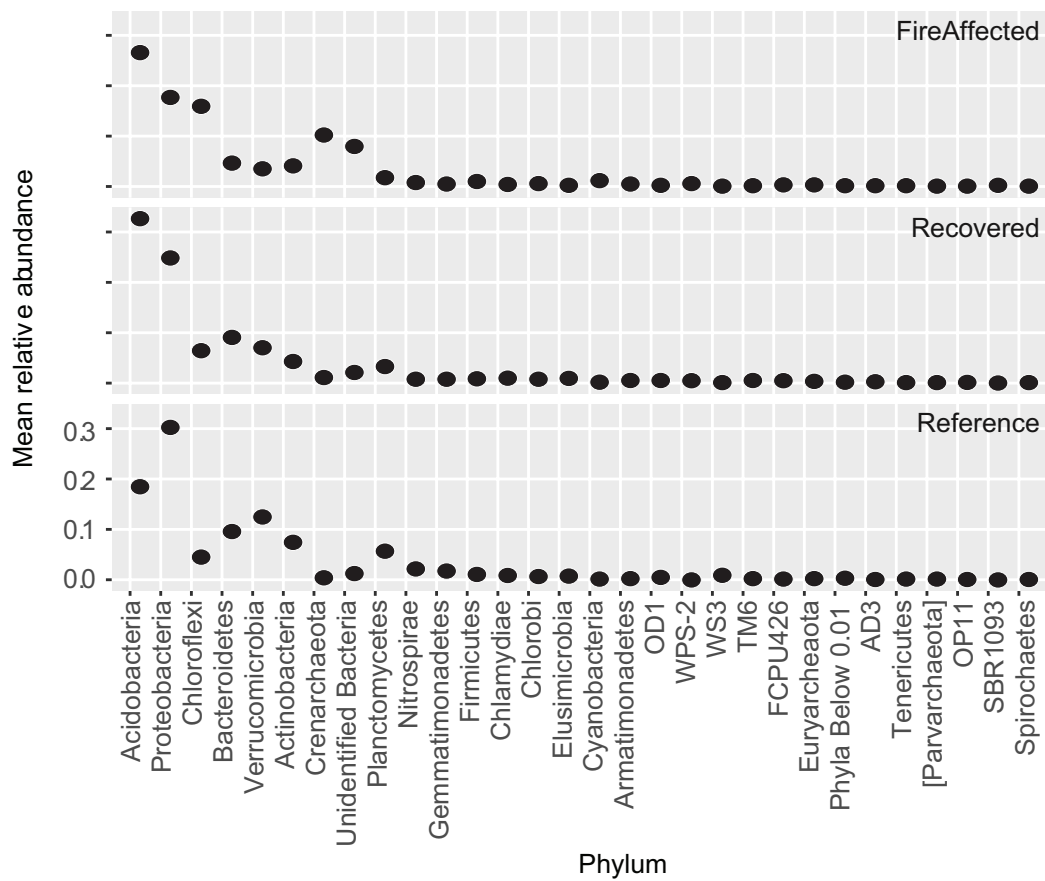


Figure 4

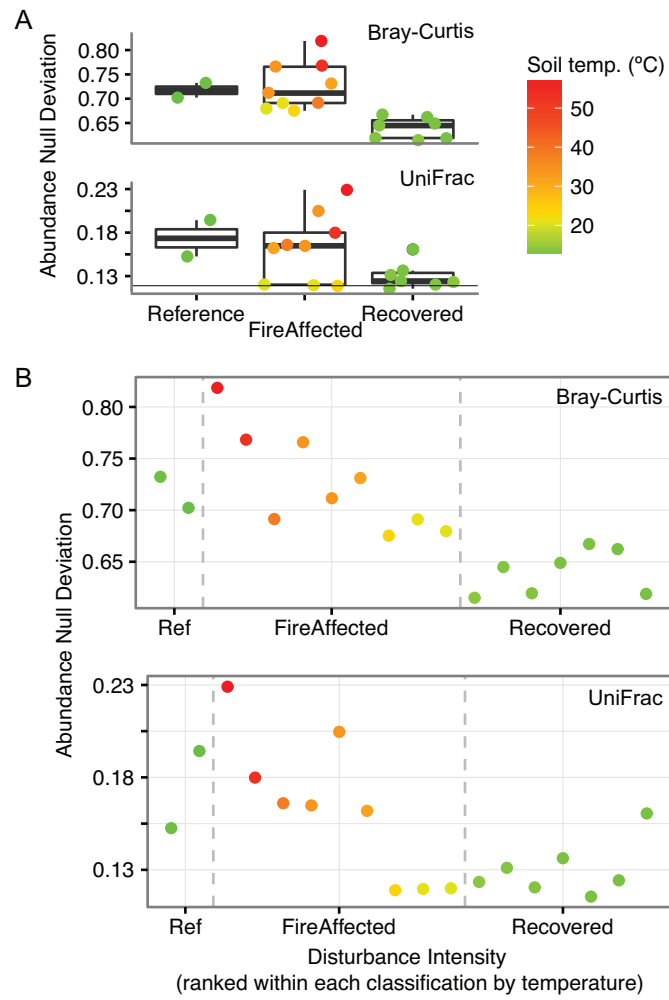


Figure 5

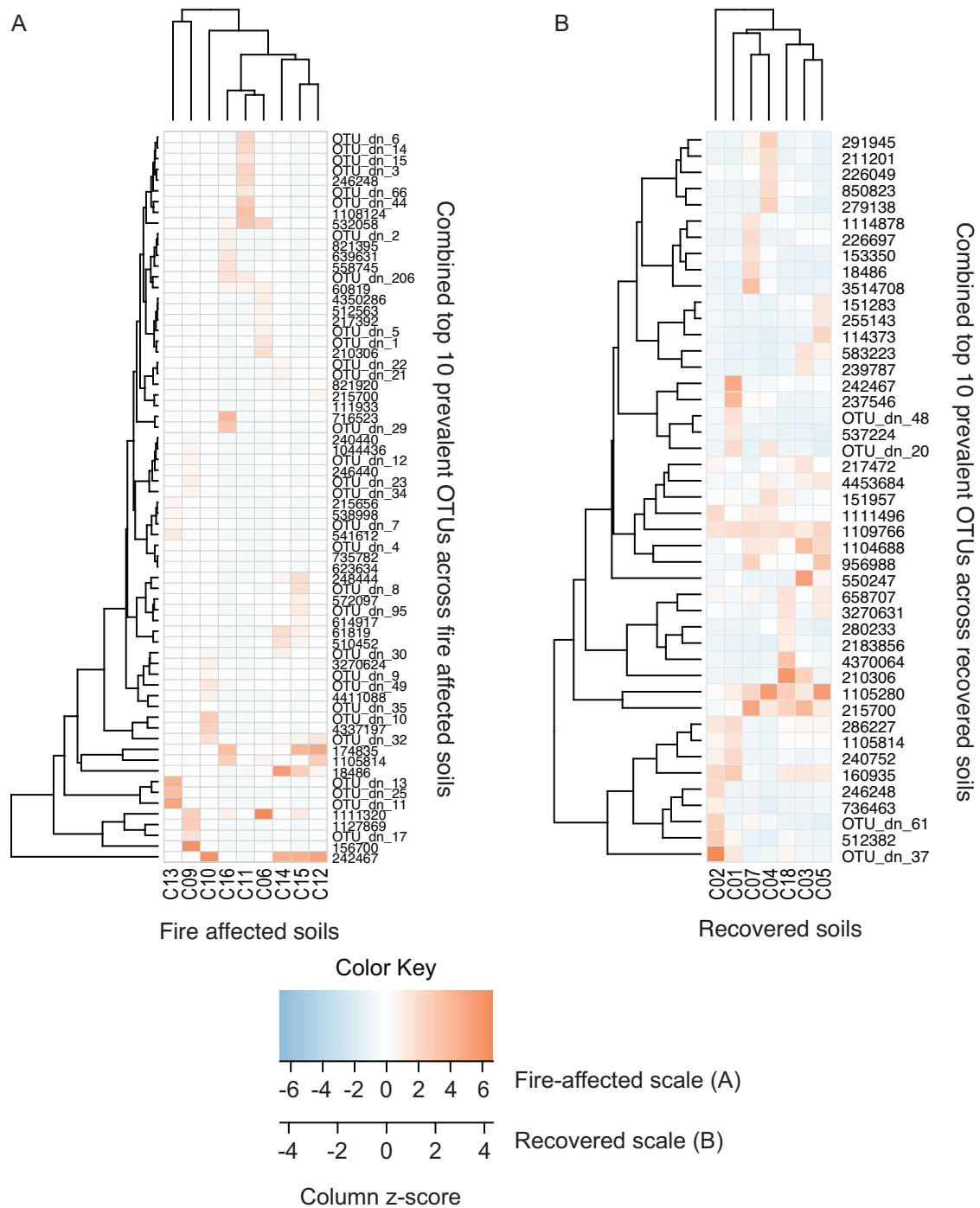
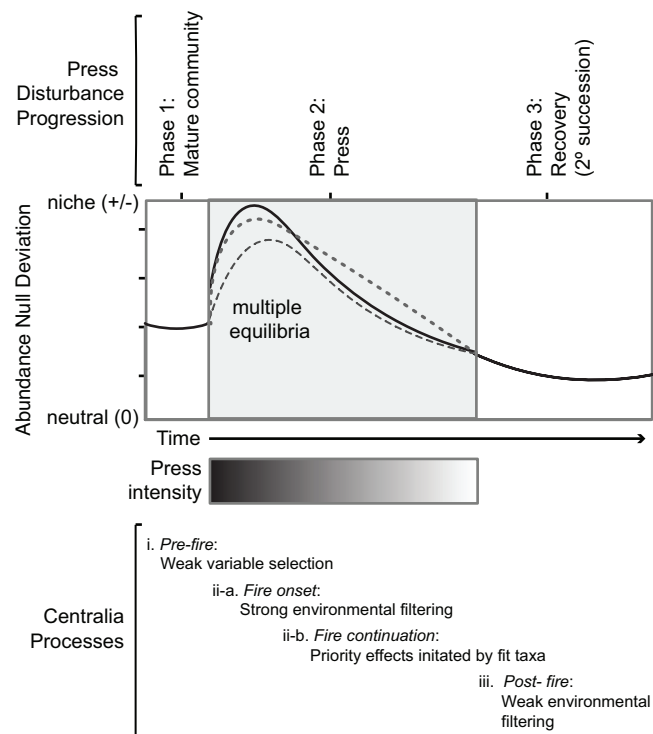


Figure 6



Tables

Table 1. Ten most abundant OTUs in fire-affected Centralia soils. OTUs (defined at 97% sequence identity) were assigned to the most resolved taxonomic level possible; there were no taxonomic assignments that could be made to these prevalent OTUs below the family level (RDP Classifier confidence > 0.80).

| OTU ID | Cumulative % abundance (out of total No. sequences in fire-affected samples) | % occurrence (out of 9 warm or venting fire-affected soils) | Taxonomic assignment |
|-----------|--|---|--|
| 111933 | 5.5% | 100% | Archaea; Crenarchaeota; MBGA |
| OTU_dn_1 | 2.5 | 100% | Bacteria; Chloroflexi; Ktedonobacteria; Thermogemmatissporales; Thermogemmatissporaceae; |
| OTU_dn_2 | 2.2 | 100% | Bacteria; Chloroflexi; Ktedonobacteria; Thermogemmatissporales Thermogemmatissporaceae |
| 242467 | 2.0 | 100% | Bacteria; Acidobacteria; DA052; Ellin6513 |
| 174835 | 2.0 | 100% | Archaea; Crenarchaeota; Thermoprotei; YNPFFA; SK322 |
| 61819 | 1.7 | 100% | Bacteria; Acidobacteria; TM1 |
| OTU_dn_17 | 1.5 | 78% | Bacteria; Proteobacteria; Deltaproteobacteria |
| 215700 | 1.4 | 100% | Bacteria; Acidobacteria; Acidobacteriia; Acidobacteriales; Koribacteraceae |
| OTU_dn_8 | 1.3 | 100% | Bacteria |
| OTU_dn_3 | 1.2 | 100% | Bacteria |